Impact of Multiple-Cell Configuration on Indoor Wireless Optical CDMA System

E. A. Alyan and S. A. Aljunid
Centre of Excellence Advanced Communication Engineering,
School of Computer and Communication Engineering (CoE ACE-SCCE),
Universiti Malaysia Perlis (UniMAP)
emadalyan@gmail.com

***Abstract*— The purpose of this study is to investigate the impact of multiple-cell configuration on indoor wireless optical CDMA system, and to develop a realistic indoor environment adding path loss along with total noises (e. g. thermal and shot noises) to the channel. A comprehensive mathematical model based on Zero Cross Correlation (ZCC) code is developed to investigate the system performance, considering the effect of received power distribution, RMS delay, and number of user on bit error rate (BER). The results are very promising, as the performances of received power, RMS delay and BER have been significantly improved by employing multi-cell configurations. For instance, the 25-cell configuration could accommodate a larger number of users even with low transmission power. It offered 283% and 52% larger cardinality at the corners and the area between the corner and the center of the room, respectively, in contrast to the 1-cell configuration.**

***Index Terms*— Indoor Communication; Multi-cell Configuration; Optical Wireless; Zero Cross Correlation (ZCC); Optical CDMA.**

I. INTRODUCTION

Unlimited customer demands such as the need for higher data rates, higher security, and increased cost effectiveness, have driven to the rapid growth of optical wireless communication (OWC) systems over RF communication systems due to the former's high transmission bandwidth [1, 2]. For the developing area of indoor OWC, energy efficiency and cost effectiveness are still viewed. In this case, LED-based communication that has attracted wide interest, is looked at in constructing the indoor OWC system. OWC systems operate at infrared frequencies (free licensed spectrum band) and can be classified into two main links as indicated by two criteria: (i) the existence of a direct path from the source to the receiver, and (ii) directionality of source beam and field of view (FOV) of the receiver [3]. These two links are the Line-of-Sight (LOS) and Non-Line-of-Sight (non-LOS). LOS links are determined by a direct path from the source to the receiver, where their beam angles are ignored, while non-LOS links mostly rely on light reflections from ceilings, walls, and other opaque objects. LOS links yield better power efficiency and lower multipath dispersion, but can suffer from shadowing due to moving objects across the direct path. Non-LOS links offer a reduction of shadowing through the use of reflected signals from ceiling, walls, and other reflecting surfaces. Nevertheless, this type of link is associated with multipath dispersion, which results in higher path losses, significant ISI and pulse spread, in contrast to LOS links. LOS and non-LOS links can also be categorized into directed, non-directed hybrid.

This paper focuses on non-directed LOS (ND-LOS) links. ND-LOS link does not require precise alignment between the source and receiver, since it has extremely good mobility and covers a larger area. Additionally, it offers lower path loss, lower ISI, and higher transmission bandwidth [4, 5]. Recently, researchers have focused on the uniform distribution of received optical power and the reduction of ISI in OWC systems. In indoor ND-LOS systems, the received power distribution and channel distortion are significantly affected by the divergence angle of the transmitter, in which lower channel distortion can be achieved using small divergence angles than those with large divergence angles [6]. Therefore, multi-cell configurations with optimum divergence angle of the transmitter are proposed for the ND-LOS systems to achieve higher transmission bandwidth and a more uniform distribution power.

ND-LOS systems also suffer from Multiple Access Interferences (MAI) and Phase-Induced Intensity Noise (PIIN) when the system has to accommodate multiple users simultaneously. Several promising technologies have been introduced in order to overcome these impairments that degrade the system performance. The optical code division multiple access (OCDMA) is one of the most attractive technologies used in the field of OWC, as multiple users can access the same bandwidth simultaneously with high level of security during transmission and reduction on the MAI [7, 8]. MAI and PIIN can be reduced or even eliminated by utilizing a good optical code set [9]. In this study, an indoor wireless optical CDMA using a Zero Cross Correlation (ZCC) code is proposed [10, 11]. The important advantage of the ZCC coding system is its capability to eliminate PIIN in order to reduce MAI due to its zero cross correlation properties. The only dominant noises that affect the signal are the thermal noise and shot noise; consequently, a better performance of BER can be achieved. Therefore, good performance in the results analyzed according to the parameters imposed will be shown, due to the avoidance of overlapping bit '1' in the ZCC code. [10].

In this paper, an optimized divergence angle of the transmitter and multi-cell configurations are developed to maximize optical received power and minimize inter-symbol interference (ISI), and thus improve the bit error rate (BER) of the system. An

indoor optical wireless system based on 4-cell and 25-cell configurations, are presented. These configurations are developed to obtain the maximum, uniform distribution of optical power received compared to the conventional 1-cell configuration. The performances of the proposed systems are examined via channel modelling in a typical room size of 5x5x3 m, respectively, in width, length and height. The effect of the severity of ISI is evaluated using RMS delay spread. A mathematical model to calculate the BER of the indoor W-OCDMA system, is also developed. The system performance is analyzed in terms of bit error rate versus the number of users for three positions, and then compared based on cell configurations.

The paper is organized as follows. In Section II, we describe the physical structure modelling. In Section III, we present the multi-path channel characteristics. In Section IV, the wireless optical CDMA (W-OCDMA) system is described. In Section V, we present some results of the received optical power; RMS delay spread; and BER performance for the proposed cell configurations. Finally, our conclusion is summarized in the Section VI.

II. System Description

A. System Configuration

In this research, three types of cell configurations for indoor ND-LOS systems are proposed to study the optical power distribution of each system on the received plane. These types are the 1-cell, 4-cell, and 25-cell configurations. Figure 1a and 1b illustrate multi-cell configurations in a room having width, length, and height of 5 m, 5m, and 3 m respectively. The ceiling is shared by the proposed cells where all cells possess an equal size in that specific ceiling. For the case of the 1-cell configuration, the distribution of the optical transmitted power

is non-uniform since the center and the edge of the room will receive the maximum and minimum power, respectively. Therefore, 4-cell and 25-cell configurations are proposed in order to achieve the maximum possible uniform optical power distribution. Nevertheless, the transmitter is centrally located at the ceiling for 1-cell configuration and at the center of each cell for 4-cell and 25-cell configurations, with a field of view (FOV) pointed towards the ground, while the receiver is located at one meter height above the floor level. Assuming that all cells in a specific configuration are having the same divergence angles and transmitted optical power.

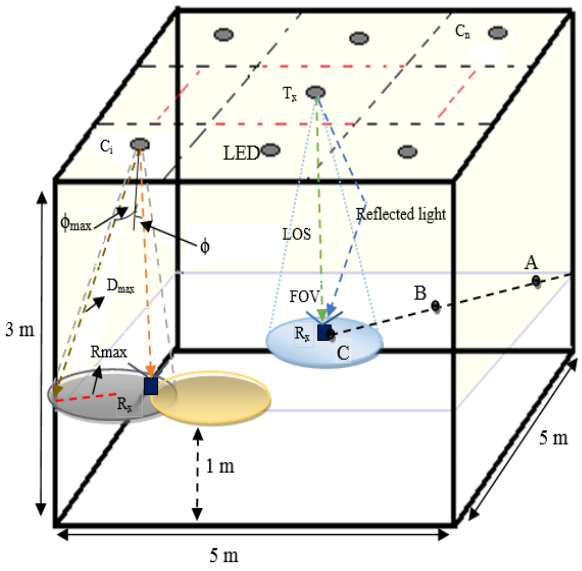

Figure 1a: Indoor ND-LOS system for multi-cell configurations.

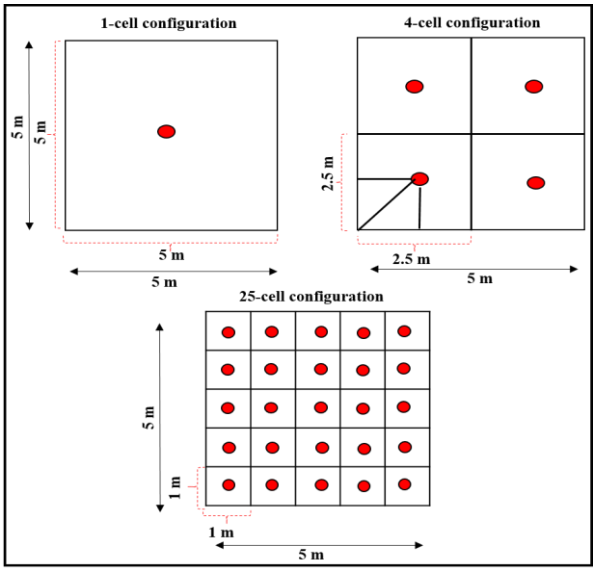

Figure 1b: Transmitters' positions on the ceiling for various cell configurations.

B. Channel Model

The LED emission can be mathematically modelled by Lambertian radiant intensity, and is presented as [5, 12, 13]:

$$R(\phi) = \frac{m+1}{2\pi}\cos^m(\phi), \quad -\frac{\pi}{2} \le \phi \le \frac{\pi}{2} \tag{1}$$

where ϕ is the incidence angle, m is the Lambertian order of emission, which is related to the half power semi-angle and represented as [12, 13]:

$$m = \frac{-\ln(2)}{\ln(\cos\phi_{1/2})} \tag{2}$$

The comparatively short length of an ND-LOS link results in a very low attenuation due to absorption and scattering. The non-directed line of sight path that exists between the transmitter and receiver, is represented by the indoor ND-LOS link. The channel DC gain for a receiver located at a distance of D and angle ϕ with respect to the transmitter, is shown in Figure 1a, and summarized in Equation (3) [5, 13]:

$$h_{los} = \begin{cases} \frac{R(\phi)}{D^2} A_R \cos(\psi), & 0 \le \psi \le \psi_C \\ 0 & \psi > \psi_C \end{cases} \tag{3}$$

As D represents distance between the transmitter and the receiver, A_R is the photodetector active area, ψ is the reception angle, ψ_c is the width of the receiver's field of view (FOV).

The overall received power resulting from the ND-LOS path of the multi transmitter system can be calculated using Equation (4):

$$P_{re} = \left(\sum_{l=1}^{\text{LEDnum}} P_t \bullet h_{los} \right) \bullet T_c(\psi) \bullet T_F(\psi) \tag{4}$$

where P_t is the transmitted optical power, $T_c(\psi)$ is the gain of the optical concentrator, $T_F(\psi)$ is the transmission coefficient of the optical filter and is given as [13]:

$$T_c(\psi) = \begin{cases} \dfrac{n^2}{\sin^2(\psi_c)} & 0 \le \psi \le \psi_c \\ 0 & \psi > \psi_c \end{cases} \tag{5}$$

n denotes the refractive index of the lens at the photodetector.

III. Multi-Path Channel Characteristics

For high data rate, the multi-path dispersion is one of the main challenging problems in indoor ND-LOS. Because it limits the overall performance of the system. Thus, by knowing the impulse channel response $h(t)$ and the RMS delay spread, the maximum available date rate can be forecasted. The impulse response for a particular transmitter and receiver in the indoor system can be expressed by Equation (6) [5, 14, 15]:

$$h^{\circ}(t) = \frac{R(\phi)}{D} A_R T_F(\psi) T_c(\psi) \cos(\psi) rect\left(\frac{\psi}{\psi_c}\right) \delta\left(t - \frac{D}{c}\right) \tag{6}$$

where c represents the speed of light, and $\delta(t - D/c)$ depicts the signal propagation delay. The step function is given by Equation (7) [5]:

$$rect\left(\frac{\psi}{\psi_c}\right) = \begin{cases} 1 & for \ \dfrac{\psi}{\psi_c} \le 1. \\ 0 & for \ \dfrac{\psi}{\psi_c} > 1. \end{cases} \tag{7}$$

The channel impulse response for multiple optical sources and multiple reflections, is given as [6]:

$$h(t) = \sum_{s=1}^{n} \left(\sum_{k=0}^{\infty} h_s^k(t) \right) \tag{8}$$

As s is the number of sources and K is the number of reflections. All reflectors are assumed to be Lambertian. The RMS delay spread is computed using the impulse response $h(t)$ as per the following Equation (9) [15, 16]:

$$D_{rms} = \left[\frac{\int (t-\mu)^2 \ h^2(t) dt}{\int h^2(t) dt} \right]^{1/2} \tag{9}$$

where μ is the mean delay spread, and calculated using Equation (10):

$$\mu = \frac{\int t h^2(t) dt}{\int h^2(t) dt} \tag{10}$$

where t is the delay time of propagation

IV. Wireless Optical CDMA (W-OCDMA)

As shown in Figure 2, the proposed system is composed of N transmitters and N receivers. Using an optical ZCC code, the information bit is first encoded for each user where many users can share the same spectrum of LEDs. Accordingly, all user signals are multiplexed and transmitted simultaneously through wireless channels. At the receiving terminal, the optical transmitted signal will be decoded using the corresponding ZCC code, then detected by the positive-intrinsic-negative (PIN) diode. [8, 17]. The following conditions are assumed to analyze the proposed system:

1) An equal transmitted and received power is assumed for each user.
2) Each light source spectrum is flat over the bandwidth $[v_0 - \Delta v/2, \ v_0 + \Delta v/2]$, in which v_0 represents the central optical frequency and Δv donates the optical source bandwidth.
3) An equal spectral width is assumed for each power spectral component.
4) Each bit stream from each user is synchronized at the receiver.

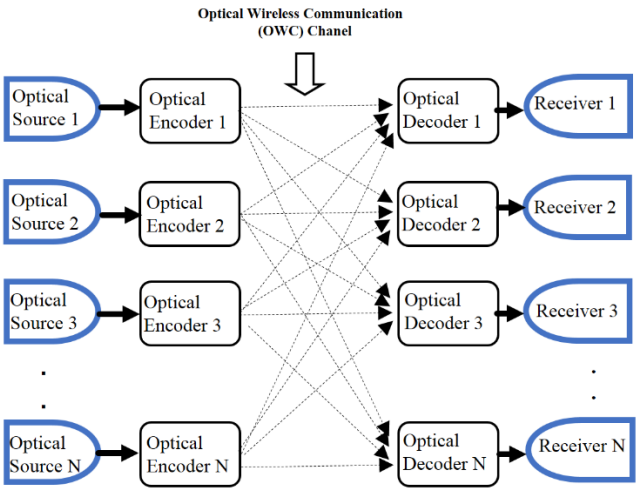

Figure 2: W-OCDMA block diagram

According to these assumptions, the transmitted optical signal is written as per Equation (11) [9]:

$$S_{tx}(t) = \sum_{n=1}^{N} P_t \; d_n(t)\, c_n(t), 0 < t < T_b \tag{11}$$

d_n is the data bit sequence of the *n-th* user, c_n is the proposed ZCC code waveform assigned to the *n-th* user, T_b is the bit duration, which is equal to L/T_c, where T_c is the chip duration of the code bit, and L is the length of the code.

The data bits will be carried by the ZCC code assigned to each user. These data bits are composed of 0 and 1, which show the absence and the availability of the optical pulse, respectively. For direct detect, the power spectral density (PSD) during one-bit duration at the photodiode can be written as per Equation (12) [18, 19]:

$$\begin{aligned} P_{rx}(\nu) &= \frac{P_{re}}{\Delta\nu} \sum_{k=1}^{C} d_k \sum_{i=1}^{N} c_x(i) c_y(i) \Pi(i) \\ &= \frac{P_{re}}{\Delta\nu} \sum_{k=1}^{C} d_k \sum_{i=1}^{N} c_x(i) c_y(i) \\ &\quad \bullet \left\{ \begin{array}{l} u\left[\nu - \nu_0 - \frac{\Delta\nu}{2L}(-L+2i-2) \right] \\ -u\left[\nu - \nu_0 - \frac{\Delta\nu}{2L}(-L+2i) \right] \end{array} \right\} \\ &= \frac{P_{re}}{\Delta\nu} \sum_{k=1}^{C} d_k \sum_{i=1}^{N} c_x(i) c_y(i) \bullet u\left[\frac{\Delta\nu}{2L} \right] \end{aligned} \tag{12}$$

where $\Delta\nu$ is the bandwidth, P_{re} is the total received power, d_k is the data bit of the *Kth* user, either "1" or "0". c_x and c_y are the two ZCC code sequences.

At the photodiode of the *n-th* receiver, the integration of the power spectral density (PSD) during one period is given as per Equation (13):

$$\begin{aligned} \int_0^{\infty} P_{rx}(\nu)\, d\nu &= \int_0^{\infty} \left(\frac{P_{re}}{\Delta\nu} \sum_{k=1}^{C} d_k \sum_{i=1}^{N} c_x(i) c_y(i) \bullet u\left[\frac{\Delta\nu}{2L} \right] \right) d\nu \\ &= \underbrace{\frac{P_{re}}{\Delta\nu}.1.w.\frac{\Delta\nu}{L}}_{auto-correlation} + \underbrace{\frac{P_{re}}{\Delta\nu}.1.0.\frac{\Delta\nu}{L}}_{cross-correlation} \\ &= \frac{P_{re}}{L}.w \end{aligned} \tag{13}$$

Utilizing the property of ZCC code [10], the value of the autocorrelation part will only be taken into consideration. Consequently, the total power incident on the photodiode is written, as per Equation (14):

$$\left\langle P_{tot}^2 \right\rangle = \Re^2 \int_0^{\infty} P_{rx}^2(\nu)\, d\nu = \frac{\Re^2 \; P_{re}^2 \; w^2}{L^2} \tag{14}$$

where $\Re$ is the photodetector responsivity and is calculated as follows $\Re = \eta q / h\nu$, with q, $h\nu$ and η as the electron charge, the photon energy and quantum efficiency, respectively.

The contribution of shot noise (σ^2_{shot}) and thermal noise ($\sigma^2_{thermal}$) resulted in the total noise power (σ^2_{tot}), which is given as per Equation (15):

$$\begin{aligned} \left\langle \sigma_{tot}^2 \right\rangle &= \left\langle \sigma_{shot}^2 \right\rangle + \left\langle \sigma_{thermal}^2 \right\rangle \\ &= \left\langle 2qBP_{tot} \right\rangle + \left\langle \frac{4KTB}{R_L} \right\rangle \\ &= \left\langle 2qB \bullet \frac{\Re \; P_{re} \; w}{L} \right\rangle + \left\langle \frac{4KTB}{R_L} \right\rangle \end{aligned} \tag{15}$$

The Phase-Induced Intensity Noise (PIIN) is neglected because of no cross correlation of bit '1' among users. The average signal-to-noise ratio (SNR) can be calculated as per Equation (16):

$$\begin{aligned} SNR &= \frac{\left\langle P_{tot}^2 \right\rangle}{\left\langle \sigma_{tot}^2 \right\rangle} \\ &= \frac{\frac{\Re^2 \; P_{re}^2 \; w^2}{L^2}}{\left\langle 2qB \bullet \frac{\Re \; P_{re} \; w}{L} \right\rangle + \left\langle \frac{4KTB}{R_L} \right\rangle} \end{aligned} \tag{16}$$

The final equation of SNR (Equation (17)) can be obtained by substituting Equation (4) into Equation (16).

where w is the weight of the code, q is the electronic charge, K is the Boltzmann's constant, L is the length of the code, B is the electrical bandwidth, T is absolute temperature, and R_L is the load resistor, which leads to the calculation of BER in Equation (18):

$$BER = 0.5 \bullet erfc\left(\sqrt{\frac{SNR}{8}} \right) \tag{18}$$

where

$$erfc(x) = \frac{2}{\sqrt{\pi}} \int_0^x e^{-t^2} dt \tag{19}$$

$$SNR = \frac{\Re^2 \bullet \left(\left(\sum_{l=1}^{\text{LEDnum}} P_t \bullet h_{los} \right) \bullet T_c(\psi) \bullet T_F(\psi) \right)^2 \bullet w^2}{L^2} \Bigg/ \left\langle 2qB \bullet \frac{\Re \bullet \left(\left(\sum_{l=1}^{\text{LEDnum}} P_t \bullet h_{los} \right) \bullet T_c(\psi) \bullet T_F(\psi) \right) \bullet w}{L} \right\rangle + \left\langle \frac{4KTB}{R_L} \right\rangle \quad (17)$$

The simulation parameters for the channel model and W-OCDMA system based on ZCC code, are listed in Table 1.

Table 1
Typical Parameters used in Mathematical Analysis

Symbol	Parameters	Values
x,y,z	room dimensions	5*m* x 5*m* x 3*m*
ρ	reflection coefficient	0.8
P	total launched power within the room (*P*)	1.0 *W*
m	lambertian Order	$m_{1\text{-cell}}$ = 0.4 $m_{4\text{-cell}}$ = 2.5 $m_{25\text{-cell}}$ = 16.0
Rx (*x*, *y*, *z*)	receiver position	A(0.5,0.5,1.0) B(1.5,1.5,1.0) C(2.5,2.5,1.0)
A_R	physical area of the photodetector	1.0 cm^2
FOV	field of view	70 [*deg.*]
$\phi_{1/2}$	semi-angle at half power per cell	$\phi_{1/2,\ 1\text{-cell}}$ = 80 [*deg.*] $\phi_{1/2,4\text{-cell}}$ = 41[*deg.*] $\phi_{1/2,25\text{-cell}}$ = 17[*deg.*]
Δx, Δy	pixel size	0.1 *m* x 0.1 *m*
T_F	gain of the optical filter	1.0
n	refractive index of the lens at the photodetector	1.5
El	elevation	90 [*deg.*]
Az	azimuth	0.0 [*deg.*]
λ_o	operating wavelength	850 *nm*
η	photodetector quantum efficiency	0.6
R_b	date bit rate	155 *Mbps*
B	electrical bandwidth	77.5 *MHz*
T	receiver noise temperature	300 *K*
R_L	receiver load resistor	1030 Ω
q	electron charge	1.6 x 10^{-19} *C*
h	Planck's constant	6.66 x 10^{-34} *J.s*
K	Boltzmann's constant	1.38 x 10^{-23} *J/K*

Configuration	Cell size	Launched power per cell (W)
1 -cell	5m x 5m	1.00
4-cell	2.5x2.5	0.25
25-cell	1x1	0.04

V. Result and Discussion

This section illustrates the mathematical analysis on the channel model and W-OCDMA based on ZCC code for 1-cell, 4-cell and 25-cell configurations of the studied system using MATLAB software. The performance of the channel model is characterized by referring to the maximum uniform distribution of the received optical power, and the reduction of ISI noise. In which, the severity of ISI can be evaluated using RMS delay spread. The quality of the signal can be expressed by bit-error rate (BER) at different receiver's positions.

A. Optical Received Power Distribution

The distribution of the optical transmitted power is non-uniform in the case of the 1-cell configuration since the maximum and minimum received power will be at the center and edges of the room, respectively. This is unlike the 4-cell and 25-cell configurations, which can achieve the maximum possible uniform optical power distribution.

As shown in Figure 3a, 3b and 3c, the received optical power from the direct path varies from -19 dBm to -28 dBm in the case of 1-cell configuration, and from -20 dBm to -26 dBm for the case of 4-cell and 25-cell configurations. It is observed that by employing multi-cell configurations, a more uniform distributed received power can be achieved, thus improving the minimum received power at the corner and edges of the room. For instance, about 74% and 84% of the receiver plane in the case of 4-cell and 25-cell respectively, has identical received power varies between -20 dBm and -21 dBm, compared to 1-cell which less than 20%. Consequently, it is seen that the 25-cell configuration has the maximum uniform received power in comparison to the 1-cell and 4-cell configurations.

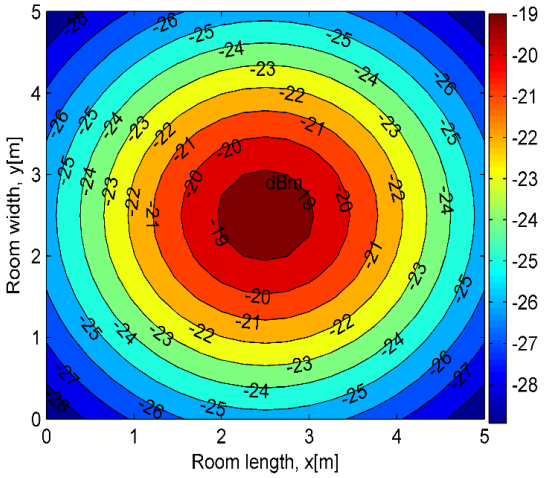

Figure 3a: Received Power (*dBm*) with consideration of 1-cell configuration

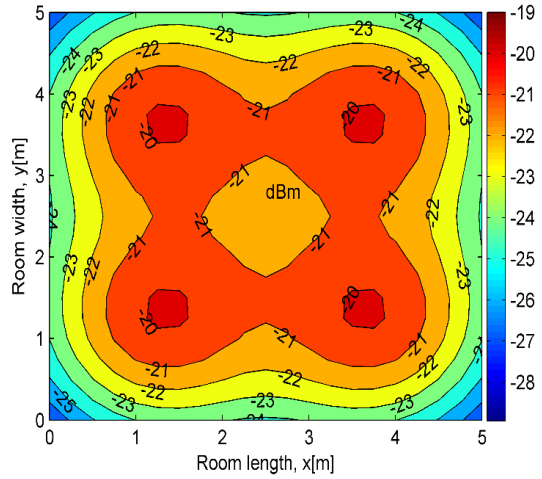

Figure 3b: Received Power (*dBm*) with consideration of 4-cell configuration

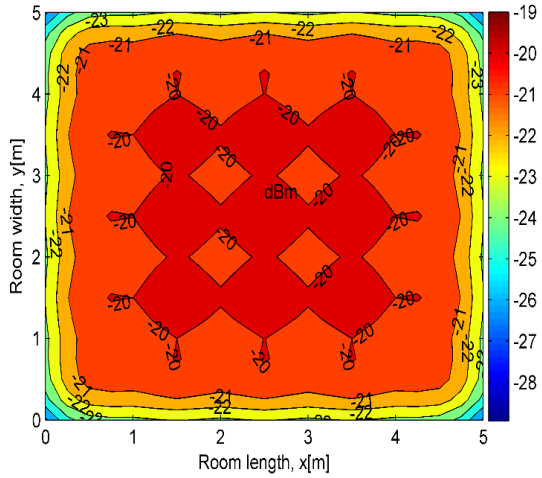

Figure 3c: Received Power (*dBm*) with consideration of 25-cell configuration

B. *RMS Delay Spread*

Figures 4a, 4b and 4c depict the RMS delay spread versus width and length of the room for measured multi-path channels at a receiver plane of one meter above the floor level. The channels with 1-cell configuration suffer from higher delay at the corners of the room due to its received power distribution, which is minimum at the corners and edges compared to the center of the room. This is unlike the 4-cell and 25-cell configurations, which induce uniform received power distribution throughout the room. Therefore, the delay at the corners and edges of the room can be reduced by employing 4-cell and 25-cell configurations. From the investigation into the channel delay dispersion for 1-cell, 4-cell and 25-cell configurations, it can be concluded that increasing the number of cells and decreasing the corresponding cell size will result in a noticeable reduction of the RMS delay spread due to the minimization of the divergence angle. The delay at the corners and edges of the room is lesser in the case of the 25-cell compared to the 4-cell and 1-cell configurations. The maximum RMS delay spreads are 0.8 *ns*, 0.7 *ns*, and 0.4 *ns* for the 1-cell, and 4-cell, and 25-cell configurations, respectively. The large multipath distortion is caused by the maximum RMS delay spread, which restricts the transmission bandwidth in the room and thus degrades the bit error rate (BER).

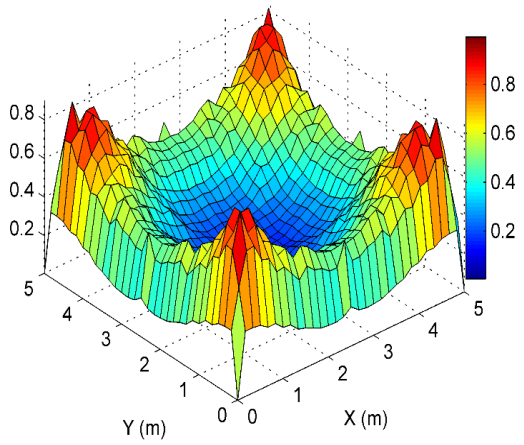

Figure 4a: RMS delay spread Spatial distribution for 1-cell configuration.

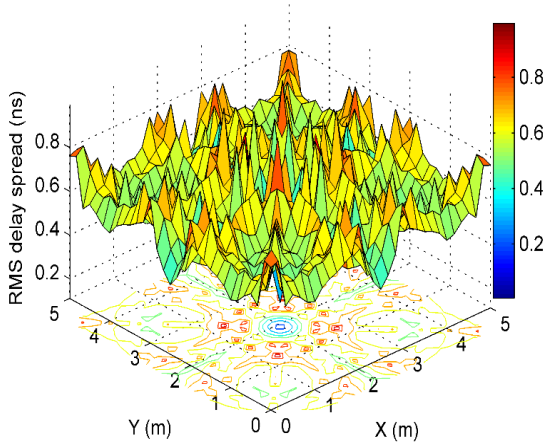

Figure 4b: RMS delay spread Spatial distribution for 4-cell configuration.

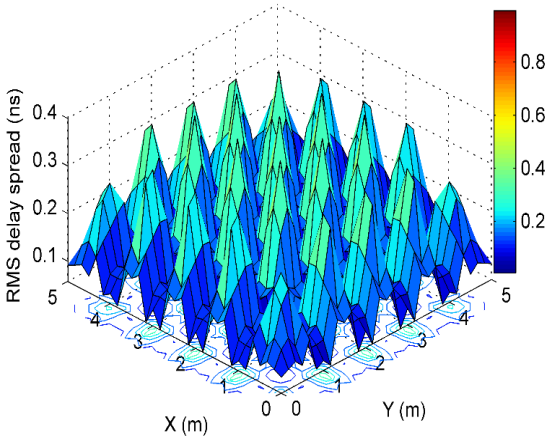

Figure 4c: RMS delay spread Spatial distribution for 25-cell configuration.

C. *Bit Error Rate Analysis*

The bit error rate (BER) of 1-cell, 4-cell, and 25-cell configurations for three different positions is studied to evaluate the overall system performance. The three positions are *A* (at the corner), *B* (in the center point between *A* and *C*), and *C* (in the center of the room). Nevertheless, different positions within the room can support different numbers of users. As shown in Figure 5a, 5b and 5c, the authors

observed a significant improvement in the performance at positions *A* and *B* when the multi-cell configuration is employed, in comparison to the 1-cell. The improvement gained is about 116.7% and 283% at *A*, and 44% and 52% at *B* when 4-cell and 25-cell configurations are respectively employed.

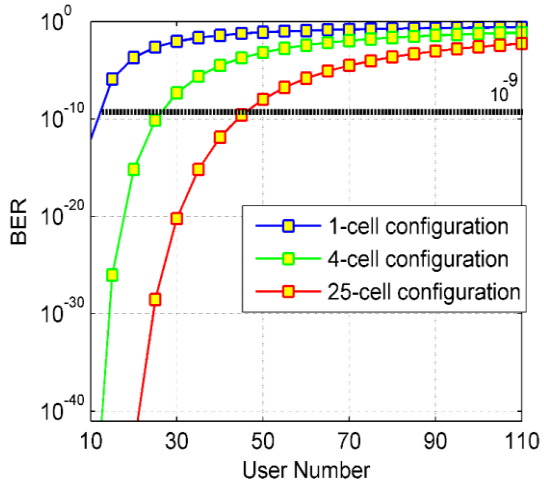

Figure 5a: BER performance for the receiver at: position A (0.5, 0.5, 1).

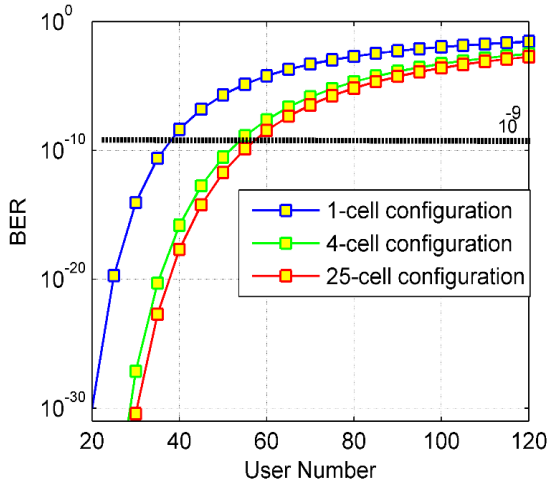

Figure 5b: BER performance for the receiver at: position B (1.5, 1.5, 1).

The results differ for position *C* where a larger number of users can be accommodated using the 1-cell configuration, in contrast to 4-cell and 25-cell configurations. Because the distribution of power in the case of 1-cell configuration is concentrated in the center where position C is located. Furthermore, by utilizing multi-cell configuration, a significant increment in the number of users is observed, particularly at the corner, and at the area between the center and the corner of the room, compared to the case of 1-cell configuration. That is to say, the increment in number of users are proportional to the increment in number of cells. The proposed system was simulated using MATLAB, and the used weight (w) for the optical ZCC code is equal to four.

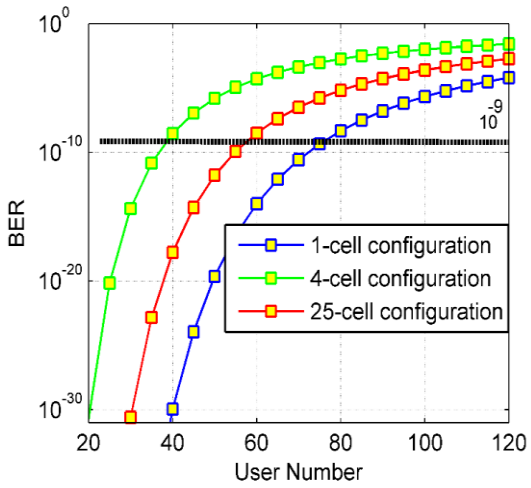

Figure 5c: BER performance of the receiver at: position C (2.5, 2.5, 1).

VI. CONCLUSION

In this research, an indoor W-OCDMA system was developed and investigated based on the ZCC code for 1-cell, 4-cell and 25-cell configurations. In which to maximize optical received power and minimize inter-symbol interference (ISI), and thus improve the bit error rate (BER) of the system. Therefore, a mathematical model to calculate the BER of the system, was also developed. The system performance was analyzed in terms of received power, RMS delay spreads and bit error rate versus the number of users, and then compared with the system based on different configurations. As a consequence of the non-uniformity of the optical transmitted power in the 1-cell configuration system, performance degradation was observed at the edges of the room due to the minimum received power. As results, the indoor W-OCDMA based on multi-cell configuration offered better performance than the 1-cell configuration system. For instance, the 25-cell configuration offered 283% and 52% larger cardinality at the corners and the area between the corner and the center of the room, respectively, in contrast to the 1-cell configuration.

REFERENCES

[1] R. Lucaciu, A. Mihăescu, and C. Vladeanu, "Dynamic OCDMA coding for indoor wireless optical communications," in *Communications (COMM), 2010 8th International Conference on* 2010, pp. 347-350.

[2] E. A. Alyan, S. Aljunid, M. Anuar, and C. Rashidi, "SAC-OCDMA over Indoor Optical Wireless Communication (OWC) System Based on Zero Cross Correlation (ZCC) Code," in *Materials Science Forum*, 2016, pp. 603-607.

[3] M. T. Alresheedi and E. J. M. H., "Hologram selection in realistic indoor optical wireless systems with angle diversity receivers," *IEEE/OSA Journal of Optical Communications and Networking*, vol. 7, pp. 797-813, 2015.

[4] N. M. Aldibbiat, Z. Ghassemlooy, and R. McLaughlin, "Indoor optical wireless systems employing dual header pulse interval modulation (DH-PIM)," *International Journal of Communication Systems*, vol. 18, pp. 285-305, 2003.

[5] Z. Ghassemlooy, W. O. Popoola, and S. Rajbhandari, *Optical Wireless Communications – System and Channel Modelling with Matlab*. USA: CRC publisher, 2012.

[6] Z. Ghassemlooy, D. Wu, M. A. Khalighi, and X. Tang, "Indoor non-directed optical wireless communications-optimization of the lambertian order," *J. Electr. Comput. Innov.*, vol. 1, pp. 1–9, 2013.

[7] C. H. Lin, J. Wu, H. W. Tsao, and C. L. Yang, "Spectral amplitude-coding optical CDMA system using Mach-Zehnder Interferometers," *Journal of Lightwave Technology*, vol. 23, pp. 1543-1555, 2005.

[8] E. A. Alyan, S. A. Aljunid, M. S. Anuar, and C. B. M. Rashidi, "Analysis of theoretical and simulated performance of indoor optical wireless system based on CDMA technology," in *3rd International Conference on Electronic Design (ICED 2016)*, 2016, pp. 164-169.

[9] L. Feng, J. Wang, R. Q. Hu, and L. Liu, "New design of optical zero correlation zone codes in quasi-synchronous VLC CDMA systems," *EURASIP Journal on Wireless Communications and Networking*, vol. 1, pp. 1-7, 2015.

[10] M. S. Anuar, S. A. Aljunid, N. M. Saad, and S. M. Hamza, "New design of spectral amplitude coding in OCDMA with zero cross-correlation," *Opt. Commun*, vol. 282, pp. 2659–2664, 2009.

[11] A. Cherifi, B. Yagoubi, B. S. Bouazza, and A. O. Dahman, "New Method for the Construction of Optical Zero Cross Correlation Code Using Block Matrices in OCDMA-OFDM System," *Journal of Telecommunication, Electronic and Computer Engineering*, vol. 8, pp. 33-39, 2016.

[12] J. R. Barry, J. M. Kahn, W. J. Krause, E. Lee, and D. G. Messerschmitt, "Simulation of multipath impulse response for indoor wireless optical channels," *Selected Areas in Communications, IEEE Journal on*, vol. 11, pp. 367-379, 1993.

[13] J. M. Kahn and J. R. Barry, "Wireless infrared communications," in *Proceedings of the IEEE*, 1997, pp. 265,298.

[14] J. B. Carruthers and S. M. Carroll, "Statistical impulse response models for indoor optical wireless channels," *International Journal of Communication Systems*, vol. 18, pp. 267-284, 2005.

[15] M. Higgins, D, , R. Green, J, , M. Leeson, S, , and E. L. Hines, "Multi-user indoor optical wireless communication system channel control using a genetic algorithm," *IET Communications*, vol. 5, pp. 937–944, 2011.

[16] B. Carruthers, S. M. Caroll, and P. Kannan, "Propagation modelling for indoor optical wireless communications using fast multi-receiver channel estimation," in *IEE Proceedings-Optoelectronics*, 2003, pp. 473-481.

[17] M. S. Anuar, S. A. Aljunid, N. M. Saad, A. Mohammed, and E. I. Babekir, "Network simulation analysis using optical Zero Cross Correlation in OCDMA system," presented at the International Conference on Intelligent and Advanced Systems, ICIAS 2007, 2007.

[18] Z. Wei, H. M. H. Shalaby, and H. Ghafouri-Shiraz, "Modified Quadratic Congruence codes for fiber bragg-grating-based spectral-amplitude-coding optical CDMA systems," *Journal of Lightwave Technology*, vol. 19, 2001.

[19] H. I. Nur, M. S. Anuar, S. A. Aljunid, and M. Zuliyana, "Innoval Zero Cross Correlation for spectral power density efficiency," presented at the Photonics (ICP), 2013 IEEE 4th International Conference, 2013.